Inorganic Chemistry
Article
Cite This: Inorg. Chem. 2019, 58, 2109−2121
pubs.acs.org/IC

Multiple Aromatic C−H Bond Activations by an Unsaturated Dirhenium Carbonyl Complex

Richard D. Adams,* Poonam Dhull, Mark D. Smith, and Jonathan D. Tedder

Department of Chemistry and Biochemistry, University of South Carolina, Columbia, South Carolina 29208, United States

Supporting Information

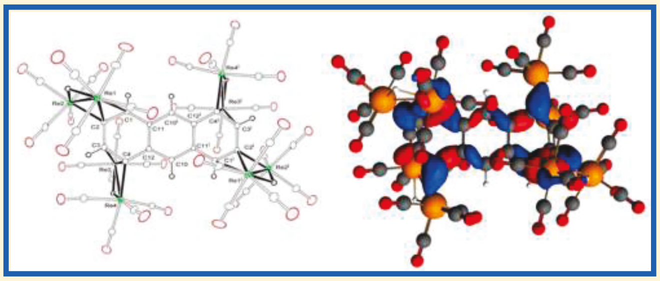

ABSTRACT: Reactions of $Re_2(CO)_8(\mu\text{-}C_6H_5)(\mu\text{-}H)$, **1**, with naphthalene and anthracene have yielded the first multiply-CH activated arene products through the reductive elimination of benzene from **1** and multiple oxidative-additions of the dirhenium octacarbonyl grouping to these polycyclic aromatic compounds under very mild conditions. In addition, compound **1** was found to react with itself to yield the bis-Re_2-metalated C_6H_4 bridged compound $Re_2(CO)_8(\mu\text{-}H)(\mu\text{-}1,\mu\text{-}3\text{-}C_6H_4)Re_2(CO)_8(\mu\text{-}H)$, **3**. Reaction of **1** with naphthalene yielded two doubly CH activated isomers, $Re_2(CO)_8(\mu\text{-}H)(\mu\text{-}\eta^2\text{-}1,2\text{-}\mu\text{-}\eta^2\text{-}3,4\text{-}C_{10}H_6)Re_2(CO)_8(\mu\text{-}H)$, **4**, 41% yield, and $Re_2(CO)_8(\mu\text{-}H)(\mu\text{-}\eta^2\text{-}1,2\text{-}\mu\text{-}\eta^2\text{-}5,6\text{-}C_{10}H_6)\text{-}Re_2(CO)_8(\mu\text{-}H)$, **5**, via the mono CH activated intermediate $Re_2(CO)_8(\mu\text{-}\eta^2\text{-}C_{10}H_7)(\mu\text{-}H)$, **2**. Compound **4** contains two $Re_2(CO)_8(\mu\text{-}H)$ groups on one C_6 ring formed by CH activations at the 2- and 4-positions. Compound **5** contains two $Re_2(CO)_8(\mu\text{-}H)$ groups; one formed by CH activation at the 2-position on one C_6 ring and the other formed by CH activation at the 6-position (or centrosymmetrically related 2′-position) on the second C_6 ring. The $Re_2(CO)_8(\mu\text{-}H)$ groups are coordinated to the C_6 rings by binuclear $\sigma + \pi$ coordination to two adjacent carbon atoms in the rings. Compound **1** reacts with anthracene to yield the mono-CH activated compound $Re_2(CO)_8(\mu\text{-}\eta^2\text{-}1,2\text{-}C_{14}H_9)(\mu\text{-}H)$, **6**, and two doubly CH activated compounds, $Re_2(CO)_8(\mu\text{-}H)(\mu\text{-}\eta^2\text{-}1,2\text{-}\mu\text{-}\eta^2\text{-}3,4\text{-}C_{14}H_8)Re_2(CO)_8(\mu\text{-}H)$, **7**, and $Re_2(CO)_8(\mu\text{-}H)(\mu\text{-}\eta^2\text{-}1,2\text{-}\mu\text{-}\eta^2\text{-}5,6\text{-}C_{14}H_8)\text{-}Re_2(CO)_8(\mu\text{-}H)$, **8**. Compounds **7** and **8** are isomers that are structurally similar to **4** and **5**. Compounds **7** and **8** can also be obtained in good yields from the reaction of **6** with **1**. In the presence of a 5/1 ratio of **1**/anthracene, a small amount (5% yield) of the tetra-substituted anthracene product $[Re_2(CO)_8(\mu\text{-}H)]_4(\mu\text{-}\eta^2\text{-}1,2\text{-}\mu\text{-}\eta^2\text{-}3,4\text{-}\mu\text{-}\eta^2\text{-}5,6\text{-}\mu\text{-}\eta^2\text{-}7,8\text{-}C_{14}H_6)$, **9**, was formed. Compound **9** contains four $\sigma + \pi$ coordinated $Re_2(CO)_8(\mu\text{-}H)$ groups formed by oxidative additions of the CH bonds of anthracene to the $Re_2(CO)_8$ groups at the 2, 4, 6, and 8 positions of the three ring system. Molecular orbital calculations have been performed for all new compounds in order to develop an understanding of the bonding of the ring systems to the $Re_2(CO)_8(\mu\text{-}H)$ groups. All new compounds were characterized by single-crystal X-ray diffraction analyses.

■ INTRODUCTION

In 1965 Chatt and Davidson reported the first example of an aromatic CH activation by the oxidative-addition one of the CH bonds of the naphthalene ligand in the ruthenium complex $Ru(Me_2PCH_2CH_2PMe_2)_2(\eta^2\text{-}C_{10}H_8)$ to the metal atom to form the complex $Ru(Me_2PCH_2CH_2PMe_2)_2(\eta^1\text{-}C_{10}H_7)(H)$.[1] Today, the activation of aromatic CH bonds by metal complexes has paved the way for the synthesis and functionalization of a wide variety of organic compounds.[2] It has proven to be one of the great achievements of modern organometallic chemistry.[3]

Despite being so widely studied, there are still very few examples of multiple oxidative addition of CH bonds of unsubstituted arenes to metal complexes.[4] The reaction of $Os_3(CO)_{10}(NCMe)_2$ with C_6H_6 is known to yield the ortho-dimetalated benzene or "benzyne" ligand complex $Os_3(CO)_9(\mu_3\text{-}\eta^2\text{-}C_6H_4)(\mu\text{-}H)_2$ by the activation to two adjacent CH bonds of the benzene molecule, Scheme 1.[4a]

Scheme 1

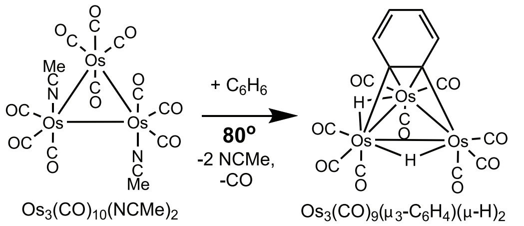

We recently reported that a second triosmium carbonyl cluster grouping could be added to the furyne ligand in the triosmium cluster complex $Os_3(CO)_9(\mu_3,\eta^2\text{-}C_4H_2O)(\mu\text{-}H)_2$ to form the bis-triosmium "furdiyne" complex $Os_3(CO)_9(\mu\text{-}H)_2(\mu_3\text{-}\eta^2\text{-}2,3\text{-}\mu_3\text{-}\eta^2\text{-}4,5\text{-}C_4O)Os_3(CO)_9(\mu\text{-}H)_2$ that has formally undergone a total of four CH bond activations on the one C_4O ring. The furdiyne ligand serves as a bridge between the two triosmium clusters, see Scheme 2.[5]

Received: November 16, 2018
Published: January 11, 2019

DOI: 10.1021/acs.inorgchem.8b03201

Scheme 2. Schematic of the Synthesis of the Compound $Os_3(CO)_9(\mu\text{-}H)_2(\mu_3\text{-}\eta^2\text{-}2,3\text{-}\mu_3\text{-}\eta^2\text{-}4,5\text{-}C_4O)Os_3(CO)_9(\mu\text{-}H)_2$ from $Os_3(CO)_9(\mu_3,\eta^2\text{-}C_4H_2O)(\mu\text{-}H)_2$

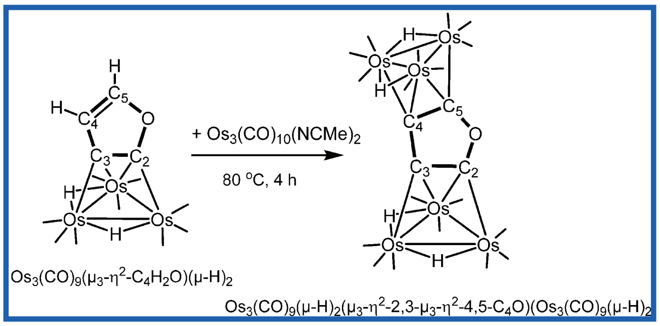

In 1984, Nubel and Brown reported the synthesis of a number of dirhenium octacarbonyl complexes containing bridging alkenyl and hydride ligands from the reaction of $Re_2(CO)_{10}$ with alkenes in the presence of UV−vis irradiation by cleavage of a CH bond in the alkene.[6] The reactions were proposed to proceed through a light-induced radical pathway. Later studies indicated that these photoreactions proceed by a decarbonylation pathway.[7] Studies of reactions of the compound $Re_2(CO)_8(thf)_2$ with alkenes and alkynes produced similar products via low temperature thermal reactions that involved facile loss of the labile thf ligands and were accompanied by CH activation pathways.[8]

In recent studies, we have obtained the remarkable dirhenium complex $Re_2(CO)_8(\mu\text{-}C_6H_5)(\mu\text{-}H)$, **1**, from the reaction of $Re_2(CO)_8(\mu\text{−}\eta^1\text{-}C_6H_5)(\mu\text{-}AuPPh_3)$ with $HSnPh_3$, Scheme 3.[9] Compound **1** contains a bridging η^1-phenyl ligand and a bridging hydrido ligand across the one and only Re−Re bond in the complex.

Interestingly, compound **1** reductively eliminates benzene and readily reacts by CH activation with other arenes, e.g., naphthalene, and even benzene itself, to undergo arene readdition by oxidative-addition, e.g., $Re_2(CO)_8(\mu\text{−}\eta^2\text{-}C_{10}H_7)(\mu\text{-}H)$, **2**, for naphthalene, Scheme 4.[10] In 2016, the mechanism for the binuclear oxidative addition of the activation of an aromatic CH bond of benzene to the dirhenium octacarbonyl grouping was established.[10]

In this Article, the first two examples of *double* CH activations in naphthalene by two sequential oxidative additions of the dirhenium complex **1** to its aromatic CH bonds are presented. There are two isomers, $Re_2(CO)_8(\mu\text{-}H)(\mu\text{−}\eta^2\text{-}1,2\text{-}\mu\text{−}\eta^2\text{-}3,4\text{-}C_{10}H_6)Re_2(CO)_8(\mu\text{-}H)$, **4**, and $Re_2(CO)_8(\mu\text{-}H)(\mu\text{−}\eta^2\text{-}1,2\text{-}\mu\text{−}\eta^2\text{-}5,6\text{-}C_{10}H_6)Re_2(CO)_8(\mu\text{-}H)$, **5**. Compound **4** contains two $Re_2(CO)_8$ groups that are coordinated in a $\sigma\text{−}\pi$ fashion on one and the same ring of the naphthalendiyl ligand, one at the 1,2-position and the other at the 3,4-position. Compound **5** contains two $\sigma\text{−}\pi$ coordinated $Re_2(CO)_8$ groups, one on each of the two rings of the naphthalendiyl ligand. Similar products were obtained for the reaction of **1** with anthracene, but we have taken the reactions of **1** with anthracene an important step further by adding four $Re_2(CO)_8$ groups to it to yield the first quadruply-CH activated anthracenetetrayl complex $[Re_2(CO)_8(\mu\text{-}H)]_4(\mu\text{−}\eta^2\text{-}1,2\text{-}\mu\text{−}\eta^2\text{-}3,4\text{-}\mu\text{−}\eta^2\text{-}5,6\text{-}\mu\text{−}\eta^2\text{-}7,8\text{-}C_{14}H_6)$. A preliminary report of this work has been published.[11]

Scheme 4. Schematic of Benzene−Naphthalene Exchange with Compound 1

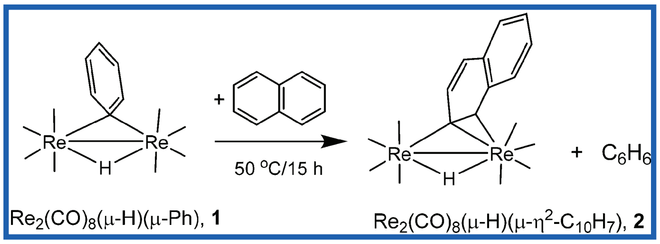

■ RESULTS AND DISCUSSION

The simplest of these dirhenium multiple-metalation CH activation reactions that we have studied is the self-condensation of **1**. When solutions of **1** in CH_2Cl_2 solvent were heated to 40 °C for 24 h, two molecules of **1** were combined with elimination of one equivalent of benzene to yield the new tetrarhenium complex, $Re_2(CO)_8(\mu\text{-}H)(\mu\text{−}\eta^1\text{-}1\text{-}\mu\text{−}\eta^1\text{-}3\text{-}C_6H_4)Re_2(CO)_8(\mu\text{-}H)$, **3**, in 51% yield, see Scheme 5.

Scheme 5. Schematic of the Synthesis of the Compound 3 from 1

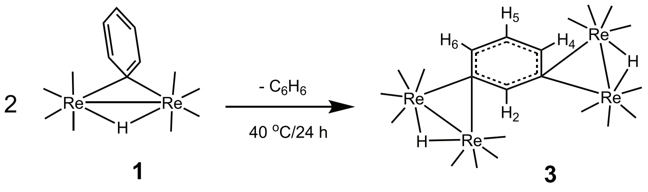

The molecular structure of **3** was established crystallographically, and an ORTEP diagram of its structure is shown in Figure 1. The complex contains two $Re_2(CO)_8(\mu\text{-}H)$ groupings bridged by a single C_6H_4 ligand.

Each $Re_2(CO)_8(\mu\text{-}H)$ group in **3** is bridged by a single carbon atom of the C_6 ring; one at the C(1) position and the other at the C(3) position. The $Re_2(CO)_8(\mu\text{-}H)$ groups are canted toward opposite sides of the ring and give the molecule and an overall approximate C_2 symmetry. The Re−C bond lengths are slightly different in length. The Re−C bond to the metal atom that lies in the plane of the ring is significantly shorter, Re(1)−C(1) = 2.224(4) Å, Re(4)−C(3) = 2.224(4) Å, than those that are out of the plane of the ring, Re(2)−C(1) = 2.417(4) Å, Re(3)−C(3) = 2.424(4) Å. The two Re−Re

Scheme 3. Schematic of the Synthesis of the Compound $Re_2(CO)_8(\mu\text{-}C_6H_5)(\mu\text{-}H)$, 1

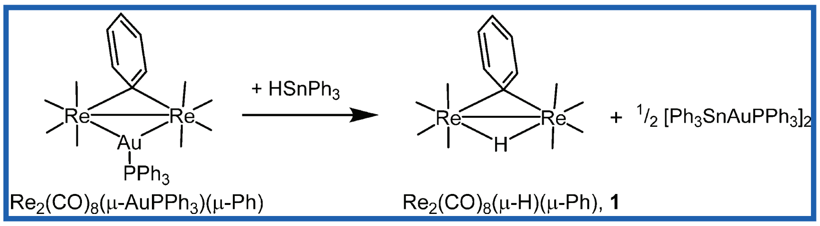

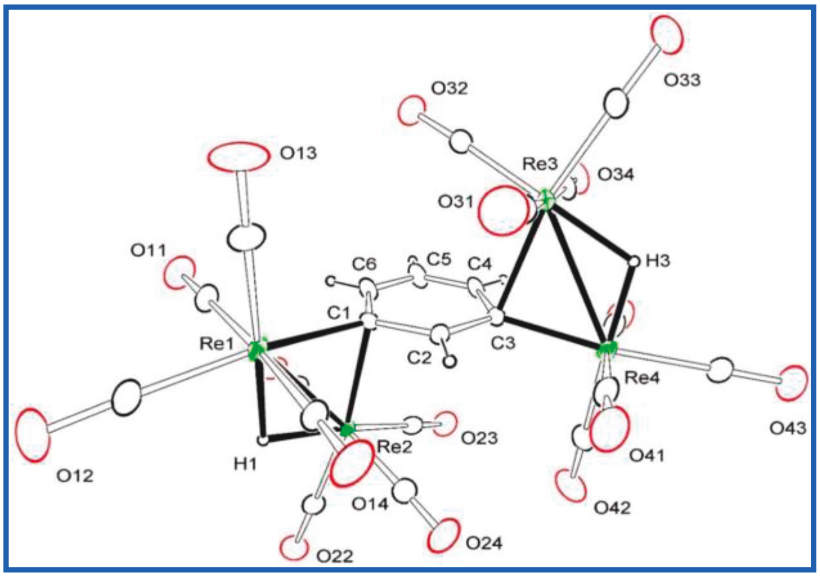

Figure 1. ORTEP diagram of the molecular structure of $Re_2(CO)_8(\mu\text{-}H)(\mu\text{-}1,\mu\text{-}3\text{-}C_6H_4)Re_2(CO)_8(\mu\text{-}H)$, **3**, showing 15% thermal ellipsoid probability. Selected interatomic bond distances (Å) are as follow: Re(1)−Re(2) = 3.0046(2), Re(3)−Re(4) = 3.0240(2), Re(1)−H(1) = 1.85(5), Re(2)−H(1) = 1.89(5), Re(3)−H(3) = 1.92(5), Re(4)−H(3) = 1.72(5), Re(1)−C(1) = 2.224(4), Re(2)−C(1) = 2.417(4), Re(3)−C(3) = 2.424(4), Re(4)−C(3) = 2.224(4), C(1)−C(2) = 1.410(5), C(2)−C(3) = 1.421(5), C(1)−C(6) = 1.431(5), C(3)−C(4) = 1.413(5), C(4)−C(5) = 1.393(6), C(5)−C(6) = 1.367(6).

bonds are similar in length, Re(1)−Re(2) = 3.0046(2) Å, Re(3)−Re(4) = 3.0240(2) Å and are similar to that found in **1**, Re−Re = 2.9924(3) Å.[9] Each Re_2 group contains a bridging hydrido ligand, and the two hydrido ligands are equivalent by the approximate C_2 symmetry of the molecule, and they exhibit one resonance at $\delta = -12.27$, in the ^1H NMR spectrum. The C_6H_4 ring formally donates only one electron to each $HRe_2(CO)_8$ grouping. As a result, each $HRe_2(CO)_8$ contains only 32 valence electrons, which is two less than the number required for an electronically saturated dinuclear metal grouping, i.e., each $HRe_2(CO)_8$ grouping is electronically unsaturated by the amount of two electrons. The C−C bond distances involving the carbon atoms in the C_6H_4 ring that are coordinated to a metal atom, C(1)−C(2) = 1.410(5) Å, C(1)−C(6) = 1.431(5) Å, C(2)−C(3) = 1.421(5) Å, C(3)−C(4) = 1.413(5) Å, are slightly longer than those that are not bonded to a metal atom, C(4)−C(5) = 1.393(6) Å, C(5)−C(6) = 1.367(6) Å. This may be caused by changes in the π-bonding in the C_6 ring due to the coordination to the metal atoms. This is further illustrated by ADF molecular orbital (MO) calculations, see Figure 2.

As expected, the ^1H NMR spectrum of **3** exhibits three resonances for C_6H_4 ring: δ = 8.68 (s,br, 1H), 8.08 (dd, 2H, ^3J = 7.2 Hz, ^4J = 1.5 Hz), 7.08 (t, 1H, H5, ^3J = 7.2 Hz). The substantial deshielding is consistent with the presence of considerable aromatic character.[12] The ^{13}C NMR spectrum exhibits four resonances for the C_6H_4 ligand, δ = 175.59(1C), 147.18(2C), 128.88(1C), and 124.56(2C), see Figure S9 in the Supporting Information. The resonance at 124.56 ppm is assigned to the metalated carbon atoms C(1) and C(3) as confirmed by their absence in a DEPT spectrum.

The reaction of **1** with naphthalene in a 3/1 ratio provided two new compounds, which are isomers: $Re_2(CO)_8(\mu\text{-}H)(\mu\text{-}\eta^2\text{-}1,2\text{-}\mu\text{-}\eta^2\text{-}3,4\text{-}C_{10}H_6)Re_2(CO)_8(\mu\text{-}H)$, **4**, 41% yield, and $Re_2(CO)_8(\mu\text{-}H)(\mu\text{-}\eta^2\text{-}1,2\text{-}\mu\text{-}\eta^2\text{-}5,6\text{-}C_{10}H_6)Re_2(CO)_8(\mu\text{-}H)$, **5**, 10% yield together with a 13% yield of compound **2**.[7] Both new products were also obtained in similar yields; **4**, 47% yield and **5**, 8% yield from the reaction of **1** with **2**. Compounds **4** and **5** were both characterized structurally by single-crystal X-ray diffraction analysis. Both compounds contain two $Re_2(CO)_8(\mu\text{-}H)$ groupings coordinated to a $C_{10}H_6$ naphthalendiyl ring system that was formed by the activation of two CH bonds, one CH bond by each $Re_2(CO)_8(\mu\text{-}H)$ grouping.

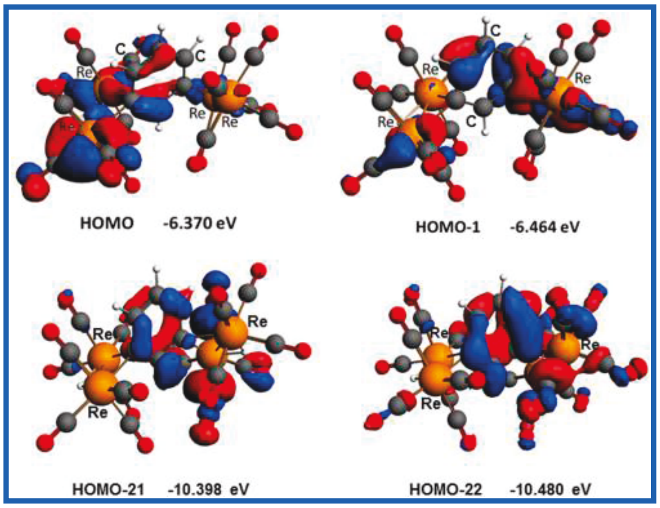

Figure 2. Selected molecular orbitals in compound **3** that show the most significant amounts of the π-bonding in the C_6 ring system. The isovalue is 0.03. The MO name and its energy in eV are given under the drawing of the corresponding orbital. Atom color code: orange = Re, gray = C, red = O, white = H.

An ORTEP drawing of its molecular structure of **4** is shown in Figure 3. Unlike compound **3**, atoms C1−C2 of the naphthalendiyl ligand are π-bonded to Re1 and atoms C3 and C4 are π-bonded to Re3. C2 is σ-bonded to Re2 and C4 is σ-bonded to Re4, which leads to the classical bridging $\eta^2\text{-}\sigma + \pi$ coordination mode to each Re_2 group as typically observed for bridging alkenyl ligands, such as found in the compound $[Re_2(CO)_8[\mu\text{-}\eta^2\text{-}HCC(H)C_4H_9]_2(\mu_4\text{-}Hg)$ that contains an

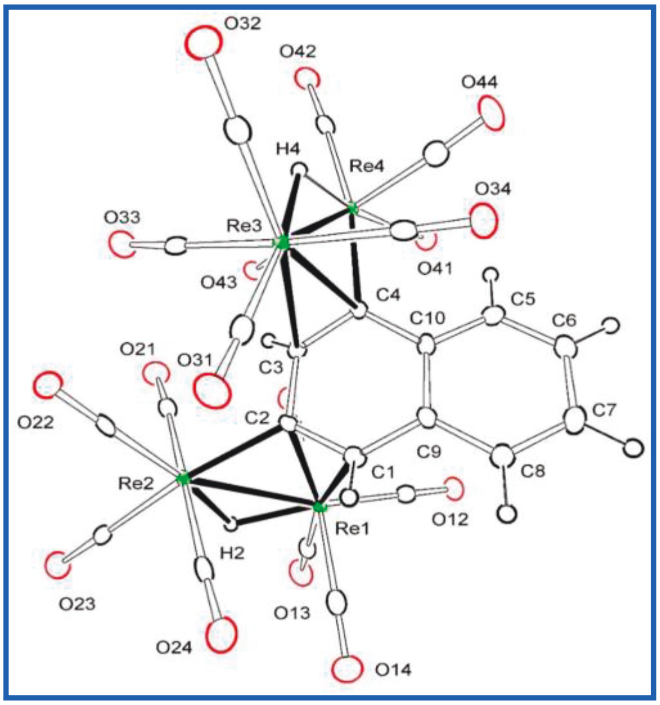

Figure 3. ORTEP diagram of the molecular structure of $[Re_2(CO)_8(\mu\text{-}H)](\mu{-}\eta^2\text{-}1,2\text{-}\mu{-}\eta^2\text{-}3,4\text{-}C_{10}H_6)[Re_2(CO)_8(\mu\text{-}H)]$, **4**, showing 50% thermal ellipsoid probability. Selected interatomic bond distances (Å) are as follow: Re(1)−Re(2) = 3.0433(2), Re(3)−Re(4) = 3.0792(2), Re(1)−H(2) = 1.88(4), Re(2)−H(2) = 1.92(4), Re(3)−H(4) = 1.78(4), Re(4)−H(4) = 1.88(4), Re(1)−C(1) = 2.526(3), Re(1)−C(2) = 2.474(3), Re(2)−C(2) = 2.201(3), Re(3)−C(3) = 2.482(3), Re(3)−C(4) = 2.489(3), Re(4)−C(4) = 2.219(3), C(1)−C(2) = 1.398(5), C(2)−C(3) = 1.476(5), C(3)−C(4) = 1.411(5), C(5)−C(6) = 1.386(5), C(6)−C(7) = 1.400(5), C(7)−C(8) = 1.375(5).

$\eta^2{-}\sigma + \pi$ bridging alkenyl ligand to each Re_2 group.[13] The CH bonds were activated at the C2 and C4 positions on the same ring in **4**. Through this $\sigma{-}\pi$ coordination, the naphthalendiyl ligand donates three electrons to each $HRe_2(CO)_8$ grouping and each Re_2 group has a total of 34 electrons, which is in accord with the 18 electron rule for each metal atom. Accordingly, the Re−Re bonds in **4**, Re(1)−Re(2) = 3.0433(2) Å and Re(3)−Re(4) = 3.0792(2) Å, are slightly longer than the unsaturated Re−Re bond in **1**, but they are similar to that in **2**, Re1−Re2 = 3.0531(3) Å, which has a similar bridging $\eta^2{-}\sigma{-}\pi$ coordination for its naphthyl ligand.[10] As found in naphthalene, the C1−C2 and the C3−C4 bond distances, C(1)−C(2) = 1.398(5) Å, C(3)−C(4) = 1.411(5) Å, in **4** are significantly shorter than the C(2)−C(3) = 1.476(5) Å distance.[14] The corresponding distances in naphthalene, the free molecule, are C(1)−C(2) = 1.365(4) Å, C(3)−C(4) = 1.377(3) Å, and C(2)−C(3) = 1.425(3) Å.[12] The shortness of the bonds in naphthalene at the C(1)−C(2) and C(3)−C(4) positions is due to a partial localization of the π-bonding at these sites. The corresponding C−C distances in the uncoordinated ring in **4** are very similar to those in naphthalene itself, C(5)−C(6) = 1.386(5) Å, C(6)−C(7) = 1.400(5) Å, C(7)−C(8) = 1.375(5) Å. The hydrido ligands in **4** are inequivalent, and two resonances were observed in its ^1H NMR spectrum, $\delta = -13.10$ and -13.63.

As found in **2**, the changes in ring bonding may be due to changes in the π-bonding network in the ring system. This is supported by geometry-optimized ADF DFT MO calculations, which show changes in the π-bonding of the complex **4** vis-à-vis that of the free molecule. Selected MOs for **4** and naphthalene itself are shown in Figure 4. As can be seen, the π-bonding in the rings in the HOMO of **4** contains a significant contribution from the HOMO−1 of naphthalene. The HOMO−1 of **4** includes a significant contribution from the HOMO of naphthalene, i.e., the bonding of the Re_2 groups to the HOMO in naphthalene is slightly better than that to the HOMO−1. The coordination of the Re_2 groups significantly distorts the π-bonding on the rings in the region of the metal−carbon bonds in both the HOMO and HOMO−1 of **4**. The HOMO−LUMO gap in **4** is 2.77 eV, see Supporting Information.

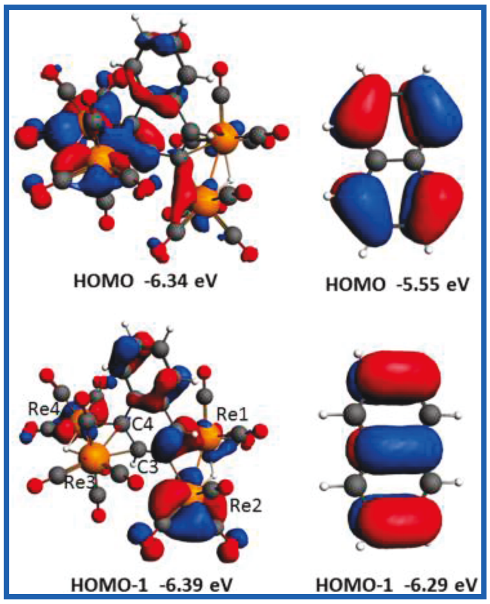

Figure 4. Selected molecular orbitals for compound **4** (HOMO and HOMO−1 on the left) and, for comparison, for naphthalene (HOMO and HOMO−1 on the right) that show significant amounts of the π-bonding in the ring systems. The isovalue is 0.05. The MO name and its energy in eV are given under the drawing of the corresponding orbital. Atom color code: orange = Re, gray = C, red = O, white = H.

An ORTEP drawing of the molecular structure of **5** is shown in Figure 5. The molecule is crystallographically centrosymmetrical having C_i molecular symmetry in the solid state. Atoms C1 and C2 of the naphthalendiyl ligand are $\eta^2{-}\sigma{-}\pi$ bonded to Re1 and Re2 in the classical bridging $\sigma{-}\pi$ coordination mode as observed in **4**, i.e., C1 and C2 are π-bonded to Re1 and C2 is σ-bonded to Re2. Atoms $C1^i$ and $C2^i$ are similarly $\eta^2{-}\sigma{-}\pi$ bonded to $Re1^i$ and $Re2^i$. In this compound the CH activations occurred on different rings of the naphthalene, namely, the 2- and 6- positions. The distribution of the C−C bond distances is similar to that observed in **2** and **4**, C(1)−C(2) = 1.406(5) Å, C(2)−C(3) = 1.450(5) Å, C(3)−C(4) = 1.363(5) Å with the uncoordinated bond C(3)−C(4) being the shortest. The equivalent Re−Re bonds in **5** are similar in length, Re(1)−Re(2) = 3.0431(2) Å, to those in **4**. The hydrido ligands in **5** are also equivalent, $\delta = -12.66$.

The nature of the bonding in the ring system in **5** was also investigated by geometry-optimized ADF DFT MO calculations. The MOs that contain the greatest amounts of π-bonding in the rings are the HOMO−10, HOMO−13,

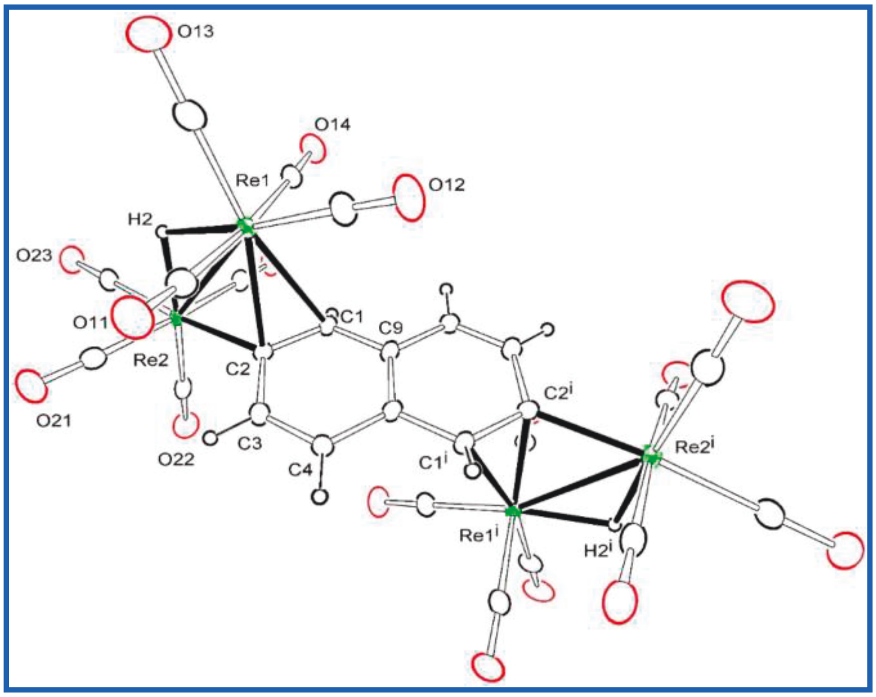

Figure 5. ORTEP diagram of the molecular structure of $[Re_2(CO)_8(\mu\text{-H})](\mu-\eta^2\text{-1,2-}\mu-\eta^2\text{-5,6-}C_{10}H_6)[Re_2(CO)_8(\mu\text{-H})]$, **5**, showing 50% thermal ellipsoid probability. Selected interatomic bond distances (Å) are as follow: Re(1)−Re(2) = 3.0431(2), Re(1)−H(2) = 1.93(4), Re(2)−H(2) = 1.87(4), Re(1)−C(1) = 2.578(3), Re(1)−C(2) = 2.448(3), Re(2)−C(2) = 2.201(3), C(1)−C(2) = 1.406(5), C(2)−C(3) = 1.450(5), C(3)−C(4) = 1.363(5).

HOMO−15, and the HOMO−20. These orbitals are shown in Figure 6.

The π-bonding in the rings in the HOMO−10 of **5** is best described as an admixture of the HOMO and HOMO−1 of naphthalene, see Figure 4 for the latter MOs. The HOMO−13 of **5** is most closely related to the HOMO−1 of naphthalene. The HOMO−15 of **5** is closely related to the HOMO−2 of naphthalene, see Figure 6 for the latter MO, and the HOMO−20 in **5** is very closely correlated to the HOMO−5 in naphthalene. The HOMO−LUMO gap in **5** is 2.76 eV.

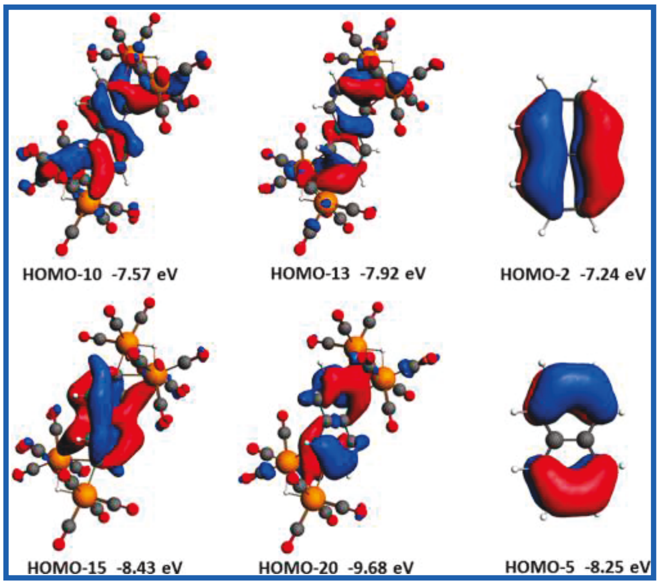

Figure 6. Selected molecular orbitals in compound **5** (center and left-hand side) and, for comparison, the naphthalene (HOMO−2 and HOMO−5, far right-hand side) that show significant contributions of π-bonding in the ring systems. The isovalue is 0.05. The MO name and its energy in eV are given under the drawing of the corresponding orbital. Atom color code: orange = Re, gray = C, red = O, white = H.

Anthracene has been one of the most difficult ring systems to engage in CH activation by oxidative-addition to metal complexes. Jones has attributed this to strong η^2-C−C coordination of the rings to metal atoms.[15] However, the reaction of $Re_2(CO)_8(\mu\text{-}C_6H_5)(\mu\text{-H})$, **1** with anthracene, $C_{14}H_{10}$, in a 1/2 ratio proceeds smoothly in CH_2Cl_2 solvent at reflux (15 h) to give the new compound $Re_2(CO)_8(\mu-\eta^2\text{-}C_{14}H_9)(\mu\text{-H})$, **6**, in 73% yield by reductive-elimination of benzene from **1** and the oxidative-addition of the CH bond at the 2-position of the anthracene to the two rhenium atoms of **1**. An ORTEP diagram of the molecular structure of **6** is shown in Figure 7.

Compound **6** contains a bridging η^2-anthracenyl, η^2-$C_{14}H_9$, ligand across the Re−Re bond of a $Re_2(CO)_8(\mu\text{-H})$ group in the classical $\sigma-\pi$ coordination mode as previously observed for the structure of **2**.[13] The mechanism of CH activation is believed to be similar to that which was determined for the formation of **2**. The C(1)−C(2) bond in **6** is π-bonded Re(1), Re(1)−C(1) = 2.571(3) Å and Re(1)−C(2) = 2.431(4) Å. Atom C(2) is σ-bonded to Re(2), Re(2)−C(2) = 2.205(4) Å. The C(1)−C(2) distance, 1.389(5) Å, is similar to that found in **2**, C(1)−C(2) = 1.403(6) Å. The C2−C3 and C3−C4 distances are long and short, C(2)−C(3) = 1.472(5) Å, C(3)−C(4) = 1.337(5) Å, as found in **2** and in anthracene itself, 1.428(1) and 1.361(1) Å, respectively.[16] The Re−Re bond distance, Re(1)−Re(2) = 3.0450(3) Å, is also very similar to that found in **2**, Re(1)−Re(2) = 3.0531(3) Å. The bridging hydrido ligand was located and refined in the analysis, δ = −13.02. We believe that the ability of the dinuclear Re_2 group to engage in π-bonding to complement the Re−C σ-bonding permits sufficient supplementary stabilization of the complex

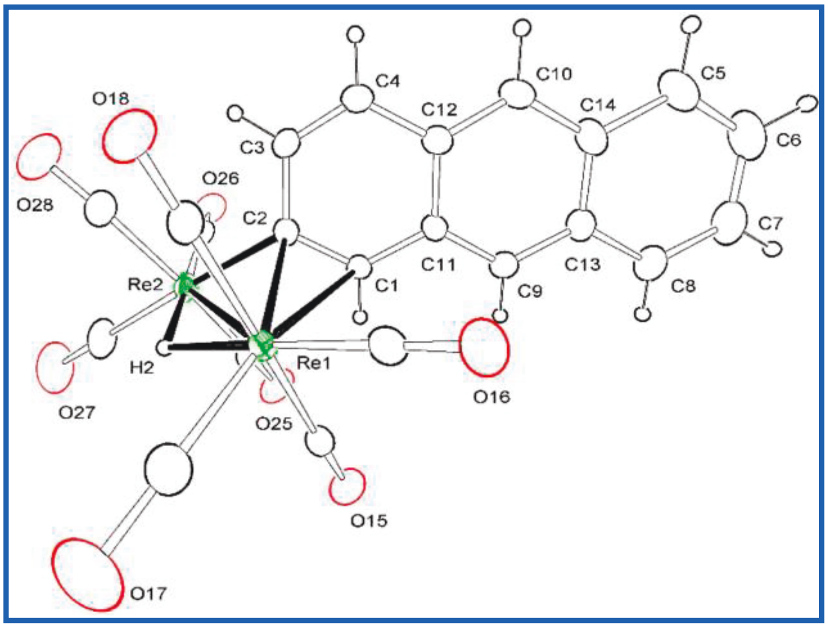

Figure 7. ORTEP diagram of the molecular structure of $Re_2(CO)_8(\mu\text{-}H)(\mu-\eta^2\text{-}1,2\text{-}C_{14}H_9)$, **6**, showing 25% thermal ellipsoid probability. Selected interatomic bond distances (Å) are as follow: Re(1)−Re(2) = 3.0450(3), Re(1)−H(2) = 1.84(5), Re(2)−H(2) = 1.76(5), Re(1)−C(2) = 2.431(4), Re(1)−C(1) = 2.571(3), Re(2)−C(2) = 2.205(4), C(1)−C(2) = 1.389(5), C(1)−C(11) = 1.446(5), C(2)−C(3) = 1.472(5), C(3)−C(4) = 1.337(5), C(4)−C(12) = 1.429(5), C(11)−C(12) = 1.423(5), C(5)−C(6) = 1.348(7), C(5)−C(14) = 1.421(5), C(6)−C(7) = 1.403(7), C(7)−C(8) = 1.354(6), C(8)−C(13) = 1.427(5), C(9)−C(11) = 1.380(5), C(9)−C(13) = 1.396(5), C(10)−C(12) = 1.386(5), C(10)−C(14) = 1.395(6), C(11)−C(12) = 1.423(5), C(13)−C(14) = 1.421(6).

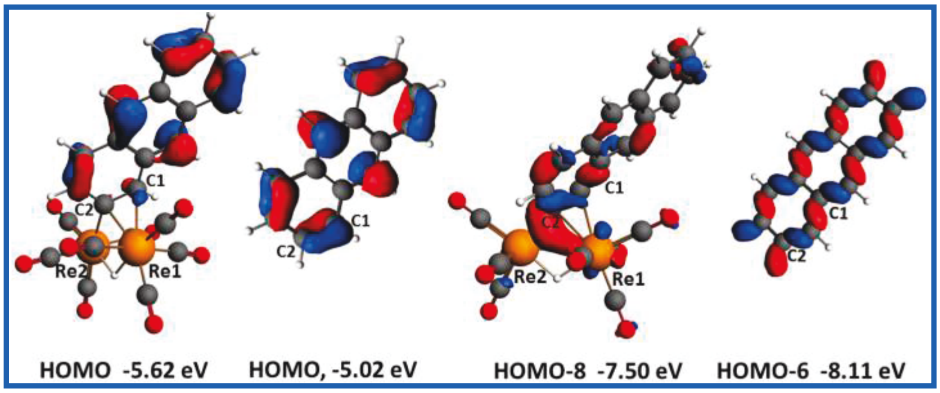

Figure 8. Selected molecular orbitals for compound **6** (HOMO far left and HOMO−8 second from right) and for anthracene (HOMO second from left and HOMO−6 far right). The isovalue is 0.05. The MO name and its energy in eV are given under the drawing of the corresponding orbital. Atom color code: orange = Re, gray = C, red = O, white = H.

to drive the reaction through the CH activation step to yield the isolable the product **6**. Complexes containing only one metal atom will not get this additional form of π-stabilization.[11] MO calculations support this notion. The HOMO of **6** and the HOMO of anthracene, the free molecule, are shown side by side in Figure 8. It can be seen that the π-bonded HOMO of anthracene serves as the basis for the π-bonding in the region of the rings in the HOMO of **6**. The nature of the σ-bonding of ring atom C2 to the Re_2 group is shown in the HOMO−8 of **6**, also shown in Figure 8. This orbital is strongly correlated to the σ-bonding HOMO−6 of anthracene. Other MOs of anthracene are supplied in the Supporting Information.

A most interesting property of the reaction of anthracene with **1** is that one can add two equivalents of **1** to the anthracene by a series of two CH activations to yield complexes similar to those obtained from the reaction of **1** with naphthalene. The reaction of **1** with anthracene, $C_{14}H_{10}$, in a 3/1 ratio yielded the new compounds: $Re_2(CO)_8(\mu\text{-}H)(\mu-\eta^2\text{-}1,2\text{-}\mu-\eta^2\text{-}3,4\text{-}C_{14}H_8)Re_2(CO)_8(\mu\text{-}H)$, **7**, 24% yield and $Re_2(CO)_8(\mu\text{-}H)(\mu-\eta^2\text{-}1,2\text{-}\mu-\eta^2\text{-}5,6\text{-}C_{14}H_8)Re_2(CO)_8(\mu\text{-}H)$, **8**, 47% yield together with a small amount of **6** in 13% yield. Compounds **7** and **8** are isomers containing two $Re_2(CO)_8(\mu\text{-}H)$ groupings, which differ by the identity of the CH bonds on the anthracene molecule, which have been activated to form them. Compounds **7** and **8** can also be obtained in 28% yield and 43% yield, respectively, from the reaction of **6** with **1**. Compounds **7** and **8** were both characterized structurally by single-crystal X-ray diffraction analyses.

An ORTEP diagram of the molecular structure of **7** is shown in Figure 9. Compound **7** contains two $Re_2(CO)_8(\mu\text{-}H)$ groupings on one and the same external C_6H_4 ring of the anthracene molecule by CH activation oxidative additions at the 2- and 4-positions. The molecule is very similar to **4** except for the replacement of the doubly metalated naphthalen-2,4-diyl group by the three ring anthracen-2,4-diyl ligand. The

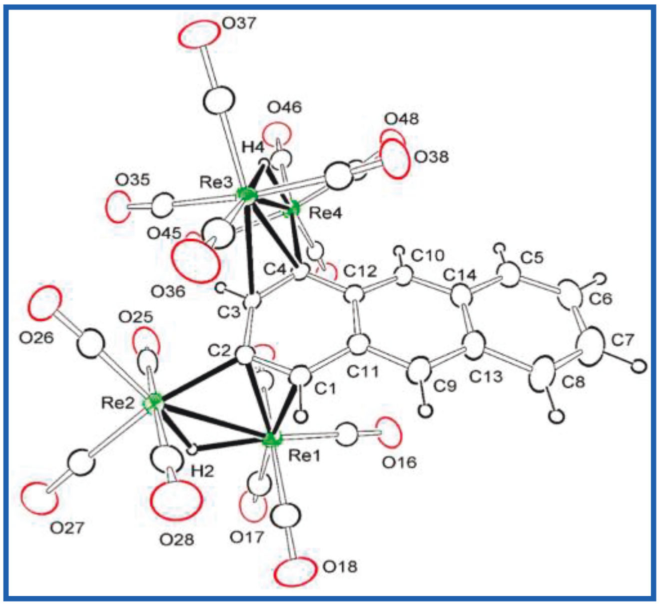

Figure 9. ORTEP diagram of the molecular structure of $[Re_2(CO)_8(\mu\text{-H})](\mu\text{-}\eta^2\text{-1,2-}\mu\text{-}\eta^2\text{-3,4-}C_{14}H_8)[Re_2(CO)_8(\mu\text{-H})]$, 7, showing 25% thermal ellipsoid probability. Selected interatomic bond distances (Å) are as follow: Re(1)−Re(2) = 3.0566(4), Re(1)−H(2) = 1.92(7), Re(2)−H(2) = 1.65(8), Re(3)−H(4) = 1.81(6), Re(4)−H(4) = 1.80(6), Re(1)−C(1) = 2.500(6), Re(1)−C(2) = 2.463(6), Re(2)−C(2) = 2.202(6), Re(3)−Re(4) = 3.0484(3), Re(3)−C(3) = 2.519(6), Re(3)−C(4) = 2.462(6), Re(4)−C(4) = 2.217(5), C(1)−C(2) = 1.383(9), C(1)−C(11) = 1.459(8), C(2)−C(3) = 1.474(8), C(3)−C(4) = 1.403(8), C(4)−C(12) = 1.470(8), C(11)−C(12) = 1.428(8).

$Re_2(CO)_8(\mu\text{-H})$ groupings in **7** are inequivalent, and two resonances are shown for the two hydrido ligands, δ = −13.15(s) and −13.68(s), in its ^1H NMR spectrum. The two π-coordinated C−C bonds, C(1)−C(2) = 1.383(9) Å and C(3)−C(4) = 1.403(8) Å are slightly longer than those in anthracene itself, 1.361(3) Å,[16] but are similar to the π-coordinated C−C bonds in **4**. Due to a decrease in π-bonding between C(2)−C(3) because of the coordination of the two neighboring C−C bonds, the C(2)−C(3) bond is the longest of all, 1.474(8) Å; however, the hydrogen atoms on atoms C1 and C3 remain highly deshielded in the ^1H NMR spectrum of **7**, δ = 7.02 (s) and 7.43 (s), respectively.

ADF DFT molecular orbital calculations were also performed on a geometry-optimized structure of **7**. The HOMO of **7** correlates favorably with the HOMO of anthracene and shows the nature of the π-bonding in the anthracendiyl ligand with the two $Re_2(CO)_8(\mu\text{-H})$ groupings to the one ring, see Figure 10. The HOMO−16 of **7** shows Re−C σ-bonding from the ring to Re(2) and Re(4). This orbital compares favorably to the σ-bonding HOMO−17 of anthracene shown to the right of it in Figure 10.

An ORTEP diagram of the molecular structure of **8** is shown in Figure 11. Compound **8** contains two $Re_2(CO)_8(\mu\text{-H})$ groupings on the external C_6H_4 rings on opposite sides of the anthracene molecule. It is similar to **5**, except for the anthracen-2,2′-diyl group located between the two $Re_2(CO)_8(\mu\text{-H})$ groupings. Similar to **5**, compound **8** is also crystallographically centrosymmetrical. CH activations occurred at the 2- and 6-positions of the anthracene molecule. The $Re_2(CO)_8(\mu\text{-H})$ groupings in **8** are equivalent, and only one resonance, a singlet at δ = −12.95, is observed for the hydrido ligands in its ^1H NMR spectrum. The Re−Re bond distance, Re(1)−Re(2) = 3.0543(18) Å, is similar to those in **5**, **6**, and **7**. Atoms C1 and C2, C(1)−C(2) = 1.404(4) Å are π-coordinated to Re1, which lies out of the plane of the ring system, Re(1)−C(1) = 2.520(3) Å, Re(1)−C(2) = 2.456(3) Å. Atom Re2 is σ-bonded to C2 at a much shorter Re−C bond distance, Re(2)−C(2) = 2.186(3) Å and lies in the plane of the rings. Because of differences in their C−C π-bonding, the uncoordinated C−C bonds on the metalated rings are quite different in length as expected, C(2)−C(3) = 1.460(4) Å and C(3)−C(4) = 1.358(4) Å, but these distances are similar in length to those found in **5**.

An ADF DFT molecular orbital analysis of **8** was also performed. Selected bonding MOs for **8** that show the nature of the bonding of the two Re_2 groups to the anthracen-2,2′-diyl ligand are shown in Figure 12. The arrangement of the ring atomic orbitals in the HOMO of **8** are very closely related to those in the HOMO of anthracene (see Figure 8) and shows the nature of the $\eta^2\text{−}\pi$ bonding interactions of the two equivalent Re(1) atoms to the rings. The HOMO−6 exhibits an important component of the Re2 to C2 σ-bonding. The HOMO−11 and HOMO−15 both show combinations of Re(2)−C(2) σ-bonding and Re(1) to C(1)−C(2) π-bonding interactions.

When compound **7** was heated to 40 °C for 40 h, small amounts of **8** were formed, but the principal products were **6**, anthracene, and $Re_2(CO)_{10}$, presumably by reductive-eliminations of the CH bonds from the "$Re_2(CO)_8$" grouping(s) that led to these decomposition products.

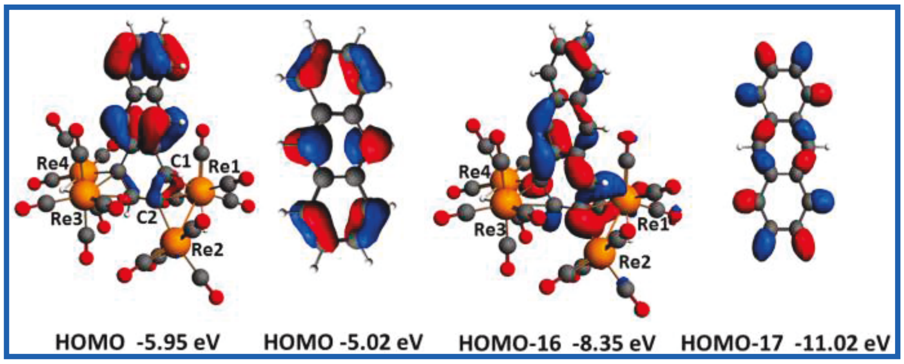

Figure 10. Selected MOs: HOMO (far left side) and HOMO−16 (second from the right side) for compound **7** and the HOMO (second from the left side) and HOMO−17 (far right side) for the anthracene ring system. The MO name and its energy in eV are given under the drawing of the corresponding orbital. The isovalue is 0.05. Atom color code: orange = Re, gray = C, red = O, white = H.

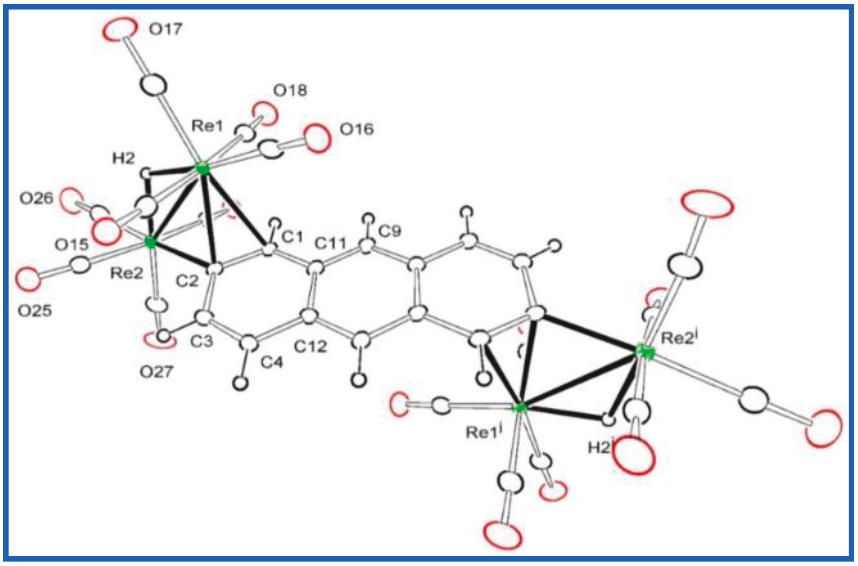

Figure 11. ORTEP diagram of the molecular structure of $[Re_2(CO)_8(\mu\text{-H})](\mu{-}\eta^2\text{-1,2-}\mu{-}\eta^2\text{-5,6-}C_{14}H_8)[Re_2(CO)_8(\mu\text{-H})]$, **8**, showing 50% thermal ellipsoid probability. Selected interatomic bond distances (Å) are as follows: Re(1)−Re(2) = 3.0543(18), Re(1)−H(2) = 1.88(6), Re(2)−H(2) = 1.85(6), Re(1)−C(2) = 2.456(3), Re(1)−C(1) = 2.520(3), Re(2)−C(2) = 2.186(3), C(1)−C(2) = 1.404(4), C(2)−C(3) = 1.460(4), C(3)−C(4) = 1.358(4).

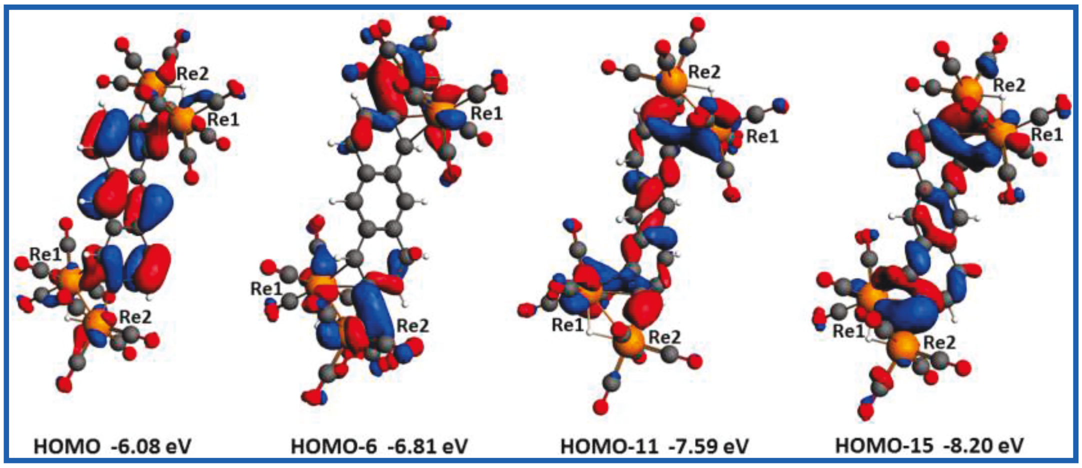

Figure 12. Selected MOs for compound **8** with their energies. The MO name and its energy in eV are given under the drawing of the corresponding orbital. The isovalue is 0.05. Atom color code: orange = Re, gray = C, red = O, white = H.

The most interesting and unexpected of all of the multiply-CH activated compounds is the quadruply metalated compound $[Re_2(CO)_8(\mu\text{-H})]_4(\mu{-}\eta^2\text{-1,2-}\mu{-}\eta^2\text{-3,4-}\mu{-}\eta^2\text{-5,6-}\mu{-}\eta^2\text{-7,8-}C_{14}H_6)$, **9**, which was obtained in only 5% yield from the reaction of **1** with anthracene in a 5/1 ratio after 24 h at 40 °C in methylene chloride solvent. Significant amounts of **7**, 24% yield, and of **8**, 33% yield, were also obtained from this reaction. The molecular structure of **9** was confirmed by a single-crystal X-ray diffraction analysis and an ORTEP diagram of its molecular structure is shown in Figure 13. Compound **9** contains four $Re_2(CO)_8(\mu\text{-H})$ groupings on the two external C_6H_4 rings of the bridging anthracen-2,2′,4,4′-tetrayl ligand with two $Re_2(CO)_8(\mu\text{-H})$ groupings on each ring. Like **8**, compound **9** is also crystallographically centrosymmetrical in the solid state. CH bond activations occurred at the 2-, 2′-, 4-, and 4′-positions of the anthracene molecule. One half of the molecule is very similar to that of **7**, which has CH bond activations at the 2-,4-positions on a single ring. One can then generate the second half of the molecule by adding a center of symmetry. The four $Re_2(CO)_8(\mu\text{-H})$ groups are grouped into two equivalent sets. Each set exhibits a single resonance for its equivalent hydrido ligands that bridge the Re−Re bonds, δ = −13.04 (s, 2H) and −13.64 (s, 2H). The Re−Re bond distances in the two sets are similar, Re(1)−Re(2) = 3.0393(4) Å, Re(3)−Re(4) = 3.0221(4) Å, and similar to those in **7** and **8**. Each $Re_2(CO)_8(\mu\text{-H})$ group is $\sigma{-}\pi$ coordinated to a pair of carbon atoms in the ring system. Re(1) is π-bonded to C(1) and C(2), Re(1)−C(1) = 2.520(7) Å and Re(1)−C(2) = 2.429(6) Å; Re(3) is π-bonded to C(3) and C(4), Re(3)−C(3) = 2.543(7) Å, Re(3)−C(4) = 2.438(7) Å. Re(2) and Re(4) are σ-bonded to C(2) and C4, respectively, with much shorter Re−C bond distances, Re(2)−C(2) = 2.202(6) Å and Re(4)−C(4) = 2.216(7) Å. The π-coordinated C−C bonds are similar in length, C(1)−C(2) = 1.388(9) Å, C(3)−C(4) = 1.417(9) Å to those in **7** and **8**. The uncoordinated C−C bond, C(2)−C(3), is very long at 1.472(10) Å, as expected, due the diminished C−C π-bonding between these atoms.

An ADF DFT molecular orbital analysis of **9** was performed, and selected bonding MOs for **9** are shown in Figure 14. The ring orbitals in the HOMO of **9** are most closely related to the

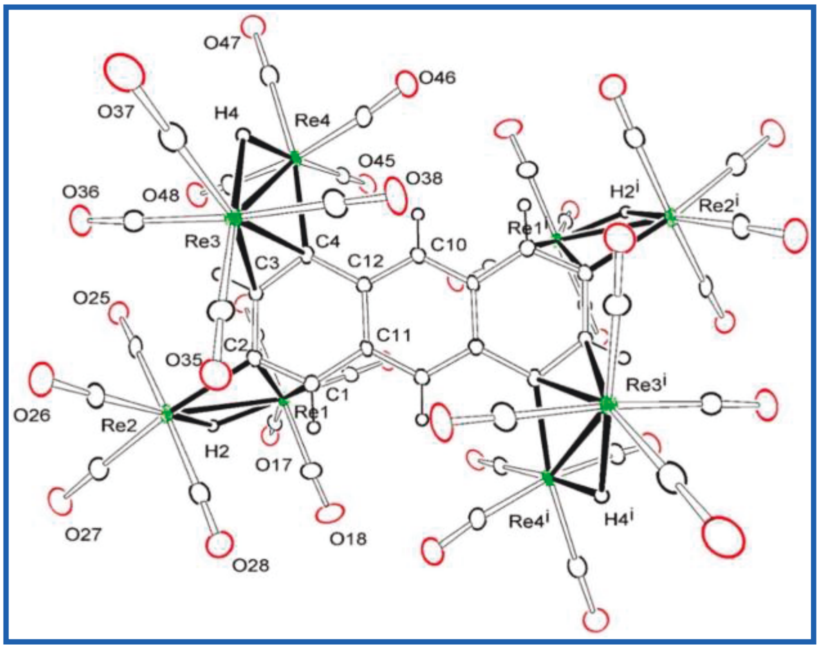

Figure 13. ORTEP diagram of the molecular structure of $[Re_2(CO)_8(\mu\text{-}H)]_4(\mu\text{–}\eta^2\text{-}1,2\text{-}\mu\text{–}\eta^2\text{-}3,4\text{-}\mu\text{–}\eta^2\text{-}5,6\text{-}\mu\text{–}\eta^2\text{-}7,8\text{-}C_{14}H_6)$, **9**, showing 30% thermal ellipsoid probability. Re(1)−Re(2) = 3.0393(4), Re(1)−H(2) = 1.80(2), Re(2)−H(2) = 1.80(2), Re(3)−H(4) = 1.78(4), Re(4)−H(4) = 1.88(4), Re(1)−C(1) = 2.520(7), Re(1)−C(2) = 2.429(6), Re(2)−C(2) = 2.202(6), Re(3)−Re(4) = 3.0221(4), Re(3)−C(3) = 2.543(7), Re(3)−C(4) = 2.438(7), Re(4)−C(4) = 2.216(7), C(1)−C(2) = 1.388(9), C(1)−C(11) = 1.445(9), C(2)−C(3) = 1.472(10), C(3)−C(4) = 1.417(9), C(4)−C(12) = 1.479(9), C(11)−C(12) = 1.424(9).

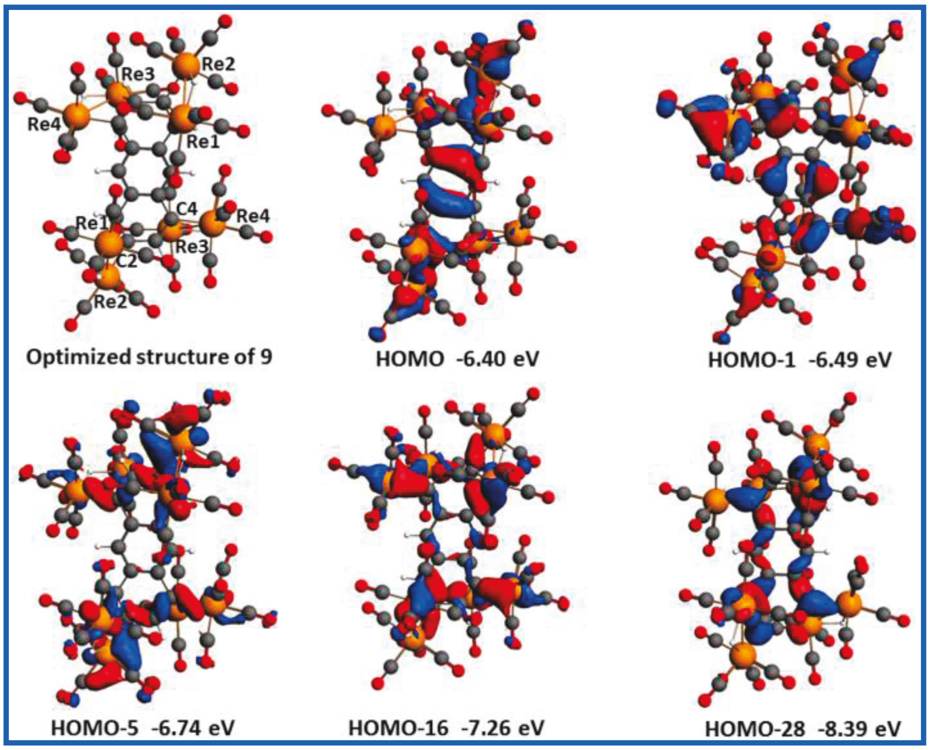

Optimized structure of 9 | HOMO -6.40 eV | HOMO-1 -6.49 eV

HOMO-5 -6.74 eV | HOMO-16 -7.26 eV | HOMO-28 -8.39 eV

Figure 14. Drawing of the geometry-optimized structure (upper left corner) and selected molecular orbitals for compound **9**. The isovalue is 0.05. The MO name and its energy in eV are given under the drawing of the corresponding orbital. Atom color code: orange = Re, gray = C, red = O, white = H.

HOMO−1 of anthracene itself (see Supporting Information). This MO shows the nature of the π-bonding of the Re(1) atoms to the C(1) and C(2) carbon atoms. The ring orbitals in the HOMO−1 of **9** are most closely related to the HOMO of anthracene and show the nature of the π-bonding of the Re(3) atoms to the C(3) and C(4) carbon atoms. The HOMO−5 shows σ-bonding between the metal atoms Re(2), Re(2^i), Re(4), and Re(4^i) and their attached carbon atoms C(2), C(2^i), C(4), and C(4^i). The ring component of the HOMO−5 is most closely related to the σ-bonding HOMO−14 orbital in anthracene itself, see Supporting Information. The lower lying HOMO−16 of **9** shows some of the Re−C σ-bonding

Scheme 6. Schematic of the Reactions of 2 with Naphthalene[a]

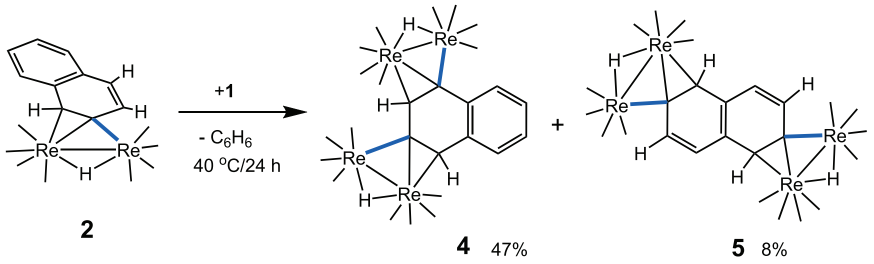

[a]The heavy blue lines show the locations of the Re−C σ-bonds. The CO ligands are represented as lines from the Re atoms.

Scheme 7. Schematic of the Reactions of 1 with Anthracene[a]

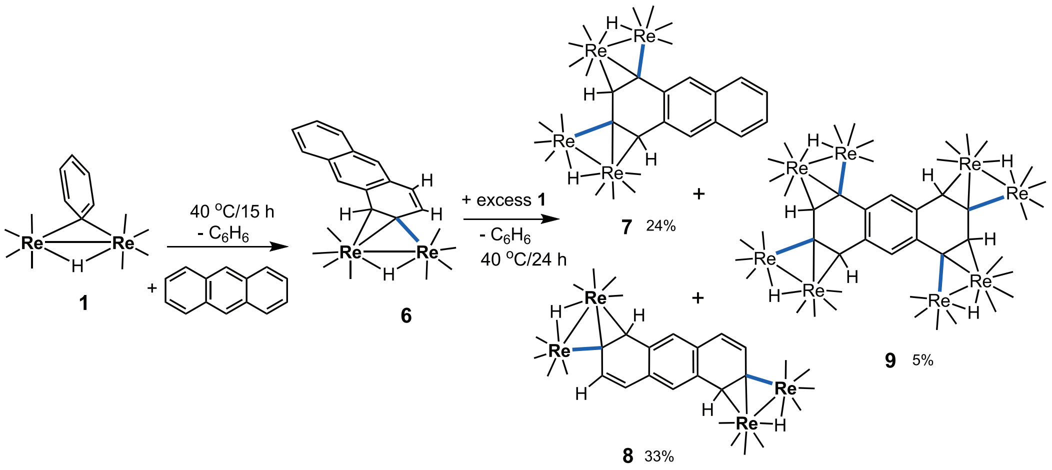

[a]The heavy blue lines show the locations of the Re−C σ-bonds. The CO ligands are represented as lines from the Re atoms.

character to Re(2)−C(2), Re(2^i)−C(2^i), Re(4)−C(4), and Re(4^i)−C(4^i). This orbital contains a significant amount of Re−C σ-bonding character and is strongly correlated to the σ-bonding HOMO−17 of the anthracene molecule, which is displayed in Figure 10. There is relatively little π-bonding to the metal atoms Re1 and Re3 in this orbital. The HOMO−28 shows σ-bonding interactions of Re(2) and Re(2^i) with atoms C(2) and C(2^i). The ring orbitals in this orbital correspond nicely with the σ-bonding HOMO−6 of anthracene (shown in Figure 8). The HOMO−LUMO gap for **9** is 2.47 eV.

■ SUMMARY AND CONCLUSIONS

A summary of the reactions and products described in this Article are shown in Schemes 5−7. Compound **1** was found to react with itself by the elimination of one equivalent of benzene to yield the doubly metalated compound **3** having meta-related $Re_2(CO)_8H$ groups. The reaction of **2** with **1** yielded two isomers of doubly CH-activated naphthalene complexes **4** and **5**. Compound **4** contains two σ−π coordinated $Re_2(CO)_8$ groups on one and the same ring of the naphthalendiyl ligand, one at the 1,2-position and the other at the 3,4-position. Compound **5** contains two σ−π coordinated $Re_2(CO)_8H$ groups, one on each of the rings of the naphthalene ligand at the 1,2- and 5,6-positions of the naphthalendiyl ligand.

Compound **1** reacts with anthracene to yield the mono-CH activated compound **6**, Scheme 7, but the reaction also yielded two doubly-CH activated products, **6** and **7**, that are similar to **4** and **5** and a small amount of the tetra-CH activated product **9** containing an anthracenetetrayl ligand when there is a sufficient excess of **1** in the reaction mixture.

All of the multiply metalated polycyclic aryl complexes exhibit strong σ-bonding to the metal atoms at the CH activation sites with important supplementary π-bonding interactions to the second metal atom in each Re_2 group. We believe that the ability of the dinuclear Re_2 group to engage in π-bonding, particularly in the anthracene derived products, to complement the Re−C σ-bonding that adds sufficient supplementary stabilization to the complex to drive through the CH activation step to yield the isolable the anthracenyl products. This type of supplementary π-bonding is not available to mononuclear metal complexes.[15] Interestingly, the doubly metalated benzene complex **3** does not show significant η^2−π bonding of the ring to the Re_2 groups. The lack of π-bonding to the metal atoms in **3** may be due to a greater degree of π-delocalization on the single C_6 ring of benzene compared to the polycyclic ring systems. The supplementary π-bonding provided by the polycyclic ring compounds brings the valence electron count for the Re_2 groups up to 34 electrons in accord with an 18 electron configuration for each metal atom, whereas the lack of π-bonding to the metal atoms in **3** leaves the Re_2 group with only 32 electrons, and they are formally electronically unsaturated. It is anticipated that multiple aromatic CH activation products as represented by compounds **2**−**5** and **7**−**9** will open the door to new pathways for the "multiple" functionalization of aromatic ring systems.

EXPERIMENTAL DETAILS

General Data. All reactions were performed under a nitrogen atmosphere by using the standard Schlenk glassware techniques. Reagent grade solvents were dried by the standard procedures and were freshly distilled prior to use. Infrared spectra were recorded on a Nicolet IS10 Midinfrared FT-IR spectrophotometer. ^{1}H NMR and ^{13}C NMR were recorded on a Bruker Advance III-HD spectrometer operating at 300 and 400 MHz, respectively. Mass spectrometric (MS) measurements performed by a direct-exposure probe by using electron impact ionization (EI) were made on a VG 70S instrument. $Re_2(CO)_{10}$ obtained from STREM and naphthalene and anthracene obtained from Sigma-Aldrich were used without further purification. $Re_2(CO)_8(\mu\text{-}C_6H_5)(\mu\text{-}H)$, **1**, was prepared according to the previously reported procedure.[9] $Re_2(CO)_8(\mu\text{-}H)(\mu{-}\eta^2\text{-}1,2\text{-}C_{10}H_7)$, **2**, was synthesized as previously reported.[10] Product separations were performed by TLC in air on Analtech 0.25 and 0.5 mm silica gel 60 Å F_{254} glass plates. X-ray intensity data for the structural analyses were measured by using a Bruker SMART APEX CCD-based diffractometer or on a Bruker D8 QUEST diffractometer equipped with a PHOTON-100 CMOS area detector and an Incoatec microfocus source using Mo Kα radiation ($\lambda = 0.71073$ Å). Crystallographic data including CCDC deposit numbers and a summary of the results of the refinements are presented in Table S1.

Preparation of $[Re_2(CO)_8(\mu\text{-}H)](\mu\text{-}1,\mu\text{-}3\text{-}C_6H_4)[Re_2(CO)_8(\mu\text{-}H)]$, 3.[8] A 25.0 mg (0.0371 mmol) amount of **1** was dissolved in 1.6 mL of CD_2Cl_2 in a 5 mm NMR tube. The NMR sample was evacuated and filled with N_2 gas. The NMR sample was then heated to 40 °C for 24 h. A ^{1}H NMR spectrum obtained after this period showed new hydride resonance at $\delta = -12.27$. The contents of the tube were then put into a flask, and the solvent was removed *in vacuo*. The residue was extracted in CH_2Cl_2 and then separated by TLC by using hexane to give a yellow band of 12.0 mg of $[Re_2(CO)_8(\mu\text{-}H)](\mu\text{-}1,\mu\text{-}3\text{-}C_6H_4)[Re_2(CO)_8(\mu\text{-}H)]$, **3**, 51% yield. Spectral data for **3**: IR ν_{CO} (cm^{-1} in CH_2Cl_2): 2107(w), 2085(m), 2020(vs), 1993(sh), 1969(sh), 1958(s). ^{1}H NMR (CD_2Cl_2, δ in ppm) 8.68 (s, br, 1H), 8.08 (dd, 2H, $^{3}J = 7.2$ Hz, $^{4}J = 1.5$ Hz), 7.08 (t, 1H, H5, $^{3}J = 7.2$ Hz), −12.27 (s, 2H, hydride). ^{13}C NMR (CD_2Cl_2, 100.66 MHz, δ in ppm): 186.28, 184.47, 184.11, 180.94, 175.59, 147.18, 128.88, and 124.56. ^{13}C NMR (CD_2Cl_2, DEPT, 100.66 MHz, δ in ppm): 175.59, 147.18, and 128.88. Mass Spec. EI/MS *m*/*z*: 1272. Elemental analysis: Calculated for $Re_4O_{16}C_{22}H_6$: C, 20.79%; H, 0.48%. Found: C, 21.68%; H, 0.47%.

Reaction of 1 with Naphthalene. A 50.0 mg (0.074 mmol) amount of **1** and 3.0 mg (0.0234 mmol) of naphthalene, $C_{10}H_8$, were dissolved in 1.6 mL of CD_2Cl_2 in a 5 mm NMR tube. The NMR sample was evacuated and filled with nitrogen. The sample was then heated to 40 °C for 24 h. A ^{1}H NMR spectrum obtained after this period showed new hydride resonances. The contents were then put into a flask, and solvent was removed *in vacuo*. The residue was extracted in CH_2Cl_2 and separated by TLC by using hexane to give a yellow band of 20.0 mg of $[Re_2(CO)_8(\mu\text{-}H)](\mu{-}\eta^2\text{-}1,2\text{-}\mu{-}\eta^2\text{-}3,4\text{-}C_{10}H_6)[Re_2(CO)_8(\mu\text{-}H)]$, **4**, 41% yield, as major product and yellow band of 5.0 mg of $[Re_2(CO)_8(\mu\text{-}H)](\mu{-}\eta^2\text{-}1,2\text{-}\mu{-}\eta^2\text{-}5,6\text{-}C_{10}H_6)\text{-}[Re_2(CO)_8(\mu\text{-}H)]$, **5**, 10% yield, along with 3.0 mg of compound **3**, 6% yield, and 7.0 mg of known compound $Re_2(CO)_8(\mu\text{-}H)(\mu{-}\eta^2\text{-}1,2\text{-}C_{10}H_7)$, **2**, 13% yield. Spectral data for **4**: IR ν_{CO} (cm^{-1} in CH_2Cl_2): 2108(m), 2084(s), 2023(vs), 1991(sh), 1976(s), 1959(sh). ^{1}H NMR (CD_2Cl_2, δ in ppm) 8.19−8.22 (m, 1H), 7.81−7.84 (m, 1H), 7.62−7.65 (m, 2H), 7.52 (d, 1H, $^{4}J = 1.5$Hs), 6.90 (s,br, 1H), −13.10 (s, 1H, hydride), and −13.63 (s, 1H, hydride). Mass Spec. EI/MS *m*/*z*: 1322, M^{+}, 1238, M^{+} − 3CO. Spectral data for **5**: IR ν_{CO} (cm^{-1} in CH_2Cl_2): 2110(m), 2084(s), 2023(vs), 1991(sh), 1969(s), 1961(sh). ^{1}H NMR (CD_2Cl_2, δ in ppm) 8.35 (d, 2H, $^{3}J = 7.2$ Hz), 7.57 (d, 2H, $^{3}J = 7.2$ Hz), 7.21 (s, 2H), −12.66 (s, 2H, hydride).

Preparation of 4 and 5 from the Reaction of 1 with 2. A 30.0 mg (0.0445 mmol) amount of **1** and 20.0 mg (0.0276 mmol) of **2** were dissolved in 1.6 mL of CD_2Cl_2 in a 5 mm NMR tube. The NMR sample was evacuated and filled with nitrogen. The NMR sample was then heated to 40 °C for 24 h. A ^{1}H NMR spectrum obtained after this period showed the hydride resonances of **4** and **5**. The contents were then put into a flask, and solvent was removed *in vacuo*. The residue was then redissolved in CH_2Cl_2 and separated by TLC by using hexane solvent to give in order of elution, a yellow band of **4**, 17.0 mg, 47% yield and a yellow band of **5**, 3.0 mg, 8% yield.

Reaction of 1 with Anthracene in 1/2 Ratio. A 30.0 mg (0.0445 mmol) amount of **1** and 14.0 mg (0.078 mmol) of anthracene, $C_{14}H_{10}$, were dissolved in 15 mL of methylene chloride. The solution was then heated to reflux for 15 h. The solution was then cooled, and the solvent was removed *in vacuo*. The residue was redissolved in CH_2Cl_2 and separated by TLC by using hexane solvent to yield a yellow band of $Re_2(CO)_8(\mu\text{-}H)(\mu{-}\eta^2\text{-}1,2\text{-}C_{14}H_9)$, **6**, 25.0 mg (73% yield). Spectral data for **6**: IR ν_{CO} (cm^{-1} in CH_2Cl_2): 2111(m), 2083(s), 2016(vs), 1989(s), 1969(vs), 1954(sh). ^{1}H NMR (CD_2Cl_2, 300 MHz, δ in ppm): 8.51 (s, 1H), 8.31 (s, 1H), 8.09−8.12 (dd, 1H, $^{3}J = 6.3$ Hz, $^{4}J = 3.3$ Hz), 8.02−8.05 (m, 2H,), 7.57−7.60 (dd, 2H, H6, H7, $^{3}J = 6.6$ Hz, $^{4}J = 3.3$ Hz), 7.43−7.46 (d, 1H, $^{3}J = 8.7$ Hz), 7.31 s,1H), −13.02 (s, 1H, H2, hydride). ^{13}C NMR (CD_2Cl_2, 100.66 MHz,δ in ppm): 186.05, 185.02, 183.66, 181.52, 146.77, 135.13, 132.72, 132.49, 130.56, 129.85, 128.18, 128.12, 127.94, 126.98, 126.61, 126.50, 126.16, and 113.02. ^{13}C NMR (CD_2Cl_2, DEPT, 100.66 MHz,δ in ppm): 146.77, 128.18, 128.12, 127.94, 126.98, 126.61, 126.50, 126.16, and 113.02. Mass Spec. EI/MS *m*/*z*: 774, M^{+}, 718, M^{+}-2CO.

Reaction of 1 with Anthracene in 3/1 Ratio. A 62.4 mg (0.0927 mmol) amount of **1** and 6.0 mg (0.033 mmol) of anthracene were dissolved in 1.6 mL of CD_2Cl_2 in a 5 mm NMR tube. The NMR sample was evacuated and filled with nitrogen gas. The NMR sample was then heated to 40 °C for 24 h. A ^{1}H NMR spectrum obtained after this period showed three new hydride resonances at $\delta = -13.15$, −13.68, and −12.94 in addition to the one of **6**. The contents were transferred to a flask, and solvent was removed *in vacuo*. The residue was then dissolved in CH_2Cl_2 and separated by TLC by using hexane solvent to give in order of elution: a yellow band of 15.0 mg of $[Re_2(CO)_8(\mu\text{-}H)](\mu{-}\eta^2\text{-}1,2\text{-}\mu{-}\eta^2\text{-}3,4\text{-}C_{14}H_8)[Re_2(CO)_8(\mu\text{-}H)]$, **7**, 24% yield, and a yellow band of 30.0 mg of $[Re_2(CO)_8(\mu\text{-}H)](\mu{-}\eta^2\text{-}1,2\text{-}\mu{-}\eta^2\text{-}5,6\text{-}C_{14}H_8)[Re_2(CO)_8(\mu\text{-}H)]$, **8**, 47% yield, along with 5.0 mg of **6**, 7% yield, and 10.0 mg of compound **3**, 17% yield. Spectral data for **7**: IR ν_{CO} (cm^{-1} in CH_2Cl_2): 2108(m), 2083(s), 2023(vs), 1990(sh), 1976(s), 1958(sh). ^{1}H NMR (CD_2Cl_2, δ in ppm) 8.67 (s, 1H), 8.28 (s, 1H), 8.26 (s, 1H), 8.08 (dd, 2H, $^{3}J = 6.3$ Hz, $^{4}J = 3.3$ Hz), 7.62 (d-d, 2H, $^{3}J = 6.3$ Hz, $^{4}J = 3.3$ Hz), 7.43 (s, 1H), 7.02 (s, 1H), −13.15 (s, 1H, H2, hydride), −13.68 (s, 1H, H4, hydride). ^{13}C NMR (CD_2Cl_2, 100.66 MHz,δ in ppm): 149.12, 141.49, 139.04, 135.87, 135.84, 133.36, 132.47, 128.54, 127.77, 127.49, 127.20, 126.85, 125.72, and 105.69. ^{13}C NMR (CD_2Cl_2, DEPT, 100.66 MHz, δ in ppm): 135.87, 128.54, 127.77, 127.49, 127.20, 126.85, 125.72, and 105.69. Mass Spec. EI/MS *m*/*z*: 1372, M^{+}, 1344, M^{+} − CO. Elemental analysis (mass %): Calculated for $Re_4O_{16}C_{30}H_{10}$: C, 26.28; H, 0.74. Found: C, 27.22; H, 1.42. Spectral data for **8**: IR ν_{CO} (cm^{-1} in CH_2Cl_2): 2110(m), 2084(s), 2019(vs), 1990(sh), 1970(s), 1958(sh). ^{1}H NMR (CD_2Cl_2, δ in ppm) 8.40 (s, 2H), 8.17 (d, 2H, $^{3}J = 8.7$ Hz), 7.54(d, 2H, $^{3}J = 8.7$ Hz), 7.33 (s, 2H), −12.95 (s, 2H, hydride). Elemental analysis (mass %): Calculated for $Re_4O_{16}C_{30}H_{10}$: C, 26.28; H, 0.74. Found: C, 26.00; H, 0.80.

Preparation of 7 and 8 from Reaction of 1 with 6. A 25.0 mg (0.0371 mmol) amount of **1** and 20.0 mg (0.0276 mmol) of **6** were dissolved in 1.6 mL of CD_2Cl_2 in a 5 mm NMR tube. The NMR sample was evacuated and filled with nitrogen. The NMR sample was then heated to 40 °C for 24 h. The contents were then put into a flask, and solvent was removed *in vacuo*. The residue was extracted in CH_2Cl_2 and separated by TLC by using hexane to give a yellow band of 10.0 mg of **7**, 28% yield and 15.0 mg of **8**, 43% yield. The yield of **7** is higher (56%) if the ratio of **1**/**6** is 1/1.

Preparation of $[Re_2(CO)_8(\mu\text{-}H)]_4(\mu{-}\eta^2\text{-}1,2\text{-}\mu{-}\eta^2\text{-}3,4\text{-}\mu{-}\eta^2\text{-}5,6\text{-}\mu{-}\eta^2\text{-}7,8\text{-}C_{14}H_6)$, 9. A 60.0 mg (0.089 mmol) amount of **1** and 3.2 mg (0.0178 mmol) of anthracene were dissolved in 1.6 mL of CD_2Cl_2 in a 5 mm NMR tube. The NMR sample was evacuated and filled with nitrogen. The NMR tube was then heated to 40 °C for 24 h. The contents were then transferred to a flask and solvent was removed *in* *vacuo*. The residue was redissolved in CH_2Cl_2 and separated by TLC by using hexane solvent to give a yellow band of 3.0 mg of $[Re_2(CO)_8(\mu\text{-}H)]_4(\mu-\eta^2\text{-}1,2\text{-}\mu-\eta^2\text{-}3,4\text{-}\mu-\eta^2\text{-}5,6\text{-}\mu-\eta^2\text{-}7,8\text{-}C_{14}H_6)$, **9**, 5% yield, along with 12.0 mg of complex **3**, 22% yield, 15.0 mg of complex **7**, 24% yield, and 20.0 mg of complex **8**, 33% yield. Spectral data for **9**: IR ν_{CO} (cm^{-1} in CH_2Cl_2): 2110(m), 2084(s), 2020(vs), 1990(sh), 1971(s), 1958(sh). ^1H NMR (CD_2Cl_2, δ in ppm) 8.59 (s, 2H), 7.44 (s, 2H), 6.77 (s, 2H,), −13.04 (s, 2H, H2, H6, hydride), −13.64 (s, 2H, H4, H8, hydride).

Thermolysis of 7 at 40 °C. A 20.0 mg (0.0146 mmol) amount of **7** was dissolved in 1.6 mL of CD_2Cl_2 in a 5 mm NMR tube. The NMR sample was evacuated and filled with nitrogen. The NMR sample was then heated to 40 °C for 40 h. ^1H NMR spectrum taken after 17 h showed hydride resonances for **6**, **8**, and anthracene, after 40 h. An ^1H NMR spectrum showed that the solution contained a mixture of **6**, **7**, **8**, and anthracene. A TLC workup provided the following amounts of the products: 4.5 mg of anthracene, 2.0 mg of compound **6**, 0.5 mg of **7**, 0.5 mg of **8**, and 3.0 mg of $Re_2(CO)_{10}$.

Computational Analyses. All calculations were performed with ADF2014 program by using the PBEsol-D3 functional with ZORA scalar relativistic correction[17] and valence triple-ζ + 2 polarization, relativistically optimized (TZ2P) Slater-type basis set, with small frozen cores. All computations are done in gas phase. This choice of computational model is based on prior testing of various functionals and basis sets.[18] The PBEsol functional, which was originally developed primarily for solids, was shown to be superior to other functionals in the PBE family in the structural parameters of large organic systems[19] and for metal clusters.[20] This is also consistent with our own testing of various functionals for the structures and relative energetics in organometallic cluster complexes.[18] The dispersion corrections by Grimme et al.[17h] were included upon additional testing once they became available in the current release of ADF. The coordinates for the initiation of the geometry-optimization refinements were obtained from the crystal structure analyses.

■ ASSOCIATED CONTENT

Supporting Information

The Supporting Information is available free of charge on the ACS Publications website at DOI: 10.1021/acs.inorgchem.8b03201.

> Details of the syntheses and characterizations of the new compounds, computational details, and selected molecular orbital diagrams (PDF)

Accession Codes

CCDC 1877208−1877211 contain the supplementary crystallographic data for this paper. These data can be obtained free of charge via www.ccdc.cam.ac.uk/data_request/cif, or by emailing data_request@ccdc.cam.ac.uk, or by contacting The Cambridge Crystallographic Data Centre, 12 Union Road, Cambridge CB2 1EZ, UK; fax: +44 1223 336033.

■ AUTHOR INFORMATION

Corresponding Author

*E-mail: adamsrd@mailbox.sc.edu.

ORCID

Richard D. Adams: 0000-0003-2596-5100

Notes

The authors declare no competing financial interest.

■ ACKNOWLEDGMENTS

This research was supported by grants 1464596 and 1764192 from the U.S. National Science Foundation.

■ REFERENCES

(1) Chatt, J.; Davidson, J. M. Tautomerism of Arene and Ditertiary Phosphine Complexes of Ruthenium(0) and Preparation of New Types of Hydrido Complexes of Ruthenium (2). *J. Chem. Soc.* **1965**, 843−855.

(2) (a) Gandeepan, P.; Müller, T.; Zell, D.; Cera, G.; Warratz, S.; Ackermann, L. 3d Transition Metals for C−H Activation. *Chem. Rev.* **2018**, DOI: 10.1021/acs.chemrev.8b00507. (b) Abrams, D. J.; Provencher, P. A.; Sorensen, E. J. Recent applications of C−H functionalization in complex natural product synthesis. *Chem. Soc. Rev.* **2018**, *47*, 8925−8967. (c) Roudesly, F.; Oble, J.; Poli, G. Metal-catalyzed CH activation/functionalization: The fundamentals. *J. Mol. Catal. A: Chem.* **2017**, *426*, 275−296. (d) Ma, W.; Gandeepan, P.; Li, J.; Ackermann, L. Recent advances in positional-selective alkenylations: removable guidance for two-fold C−H activation. *Org. Chem. Front.* **2017**, *4*, 1435−1467. (e) Wedi, P.; van Gemmeren, M. Arene-Limited Nondirected C-H Activation of Arenes. *Angew. Chem., Int. Ed.* **2018**, *57*, 13016−13027. (f) Yang, Y.; Lan, J.; You, J. Oxidative C−H/C−H Coupling Reactions between Two (Hetero)arenes. *Chem. Rev.* **2017**, *117*, 8787−8863. (g) Liu, C.; Yuan, J.; Gao, M.; Tang, S.; Li, W.; Shi, R.; Lei, A. Oxidative Coupling between Two Hydrocarbons: An Update of Recent C−H Functionalizations. *Chem. Rev.* **2015**, *115*, 12138−12204. (h) Ashenhurst, J. A. Intermolecular Oxidative Cross-Coupling of Arenes. *Chem. Soc. Rev.* **2010**, *39*, 540−548. (i) Yeung, C. S.; Dong, V. M. Catalytic Dehydrogenative Cross-Coupling: Forming Carbon−Carbon Bonds by Oxidizing Two Carbon−Hydrogen Bonds. *Chem. Rev.* **2011**, *111*, 1215−1292. (j) Colby, D. A.; Bergman, R. G.; Ellman, J. A. Rhodium-Catalyzed C-C Bond Formation via Heteroatom-Directed C-H Bond Activation. *Chem. Rev.* **2010**, *110*, 624−655. (k) Daugulis, O.; Do, H. Q.; Shabashov, D. Palladium- and Copper-Catalyzed Arylation of Carbon-Hydrogen Bonds. *Acc. Chem. Res.* **2009**, *42*, 1074−1086. (l) Gensch, T.; Hopkinson, M. N.; Glorius, F.; Wencel-Delord, J. Mild metal-catalyzed C−H activation: examples and concepts. *Chem. Soc. Rev.* **2016**, *45*, 2900−2936. (m) Foley, N. A.; Lee, J. P.; Ke, Z.; Gunnoe, T. B.; Cundari, T. R. Ru(II) Catalysts Supported by Hydridotris(pyrazolyl)borate for the Hydroarylation of Olefins: Reaction Scope, Mechanistic Studies, and Guides for the Development of Improved Catalysts. *Acc. Chem. Res.* **2009**, *42*, 585−597. (n) Arockiam, P. B.; Bruneau, C.; Dixneuf, P. Ruthenium(II)-Catalyzed C−H Bond Activation and Functionalization. *Chem. Rev.* **2012**, *112*, 5879−5918. (o) Shan, C.; Zhu, L.; Qu, L. B.; Bai, R.; Lan, Y. Mechanistic view of Ru-catalyzed C−H bond activation and functionalization: computational advances. *Chem. Soc. Rev.* **2018**, *47*, 7552−7576.

(3) (a) Balcells, D.; Clot, E.; Eisenstein, O. C-H Bond Activation in Transition Metal Species from a Computational Perspective. *Chem. Rev.* **2010**, *110*, 749−823. (b) Jones, W. D. Isotope Effects in C-H Bond Activation Reactions by Transition Metals. *Acc. Chem. Res.* **2003**, *36*, 140−146. (c) Jones, W. D.; Feher, F. J. Comparative Reactivities of Hydrocarbon C-H Bonds with a Transition-Metal Complex. *Acc. Chem. Res.* **1989**, *22*, 91−100.

(4) (a) Goudsmit, R. J.; Johnson, B. F. G.; Lewis, J.; Raithby, P. J.; Rosales, M. J. Some Reactions of $[Os_3(CO)_{10}(NCMe)_2]$ with Arenes; the Molecular Structure of $[Os_3H_2(CO)_{10}(C_6H_4)]$. *J. Chem. Soc., Dalton Trans.* **1983**, 2257−2261. (b) Takao, T.; Moriya, M.; Kajigaya, M.; Suzuki, H. Direct Arylation of a Cluster-Bound Alkyne Ligand with Benzene. *Organometallics* **2010**, *29*, 4770−4773. (c) Moriya, M.; Tahara, A.; Takao, T.; Kajigaya, M.; Suzuki, H. Arylation of Hydrocarbyl Ligands Formed from *n*-Alkanes through C−H Bond Activation of Benzene Using a Triruthenium Cluster. *Eur. J. Inorg. Chem.* **2009**, *2009*, 3393−3397. (d) McGhee, W. D.; Hollander, F. J.; Bergman, R. G. C-H Oxidative Addition and Reductive Elimination Reactions in a Dinuclear Iridium Complex. *J. Am. Chem. Soc.* **1988**, *110*, 8428−8443.

(5) Adams, R. D.; Kiprotich, J.; Smith, M. D. Multiple Cluster CH Activations and Transformations of Furan by Triosmium Carbonyl Complexes. *Chem. Commun.* **2018**, *54*, 3464−3467.

(6) Nubel, P. O.; Brown, T. L. Photolysis of $Re_2(CO)_{10}$ in the Presence of Simple Olefins. Thermal Reactivity of (μ-Hydride)(μ-alkeny1)dirhenium Octacarbonyl Compounds. *J. Am. Chem. Soc.* **1984**, *106*, 644–652.

(7) Sarakha, M.; Cozzi, M.; Ferraudi, G. Mechanism of (μ-H)(μ-alkenyl)$Re_2(CO)_8$ Formation in 350 nm Flash Irradiations of $Re_2(CO)_{10}$. *Inorg. Chem.* **1996**, *35*, 3804–3807.

(8) Carlucci, L.; Proserpio, D. M.; D'Alfonso, G. 1,2-*eq,eq*-[$Re_2(CO)_8(thf)_2$]: A Reactive $Re_2(CO)_8$ Fragment That Easily Activates H-H and C-H Bonds. *Organometallics* **1999**, *18*, 2091–2098.

(9) Adams, R. D.; Rassolov, V.; Wong, Y. O. Facile C-H Bond Formation by Reductive Elimination at a Dinuclear Metal Site. *Angew. Chem., Int. Ed.* **2014**, *53*, 11006–11009.

(10) Adams, R. D.; Rassolov, V.; Wong, Y. O. Binuclear Aromatic C-H Bond Activation at a Dirhenium Site. *Angew. Chem., Int. Ed.* **2016**, *55*, 1324–1327.

(11) Adams, R. D.; Dhull, P.; Tedder, J. D. Multiple Aromatic C-H Bond Activations by a Dirhenium Carbonyl Complex. *Chem. Commun.* **2018**, *54*, 3255–3257.

(12) Mitchell, R. H. Measuring Aromaticity by NMR. *Chem. Rev.* **2001**, *101*, 1301–1315.

(13) Adams, R. D.; Wong, Y. O. New rhenium carbonyl cluster complexes containing bridging hydrocarbyl and bridging mercury groups. *J. Organomet. Chem.* **2015**, *784*, 109–113.

(14) Matsumoto, A.; Suzuki, M.; Hayashi, H.; Kuzuhara, D.; Yuasa, J.; Kawai, T.; Aratani, N.; Yamada, H. Aromaticity Relocation in Perylene Derivatives upon Two-Electron Oxidation To Form Anthracene and Phenanthrene. *Chem. - Eur. J.* **2016**, *22*, 14462–14466.

(15) Chin, R. M.; Dong, L.; Duckett, S. B.; Partridge, M. G.; Jones, W. D.; Perutz, R. N. Control of η^2-Coordination vs C-H Bond Activation by Rhodium: The Role of Aromatic Resonance Energies,. *J. Am. Chem. Soc.* **1993**, *115*, 7685–7695.

(16) Brock, C. P.; Dunitz, J. D. Temperature Dependence of Thermal Motion in Crystalline Anthracene. *Acta Crystallogr., Sect. B: Struct. Sci.* **1990**, *B46*, 795–806.

(17) (a) te Velde, G.; Bickelhaupt, F. M.; van Gisbergen, S. J. A.; Fonseca Guerra, C.; Baerends, E. J.; Snijders, J. G.; Ziegler, T. *J. Comput. Chem.* **2001**, *22*, 931–967. (b) Fonseca Guerra, C.; Snijders, J. G.; te Velde, G.; Baerends, E. *Theor. Chem. Acc.* **1998**, *99*, 391–403. (c) Perdew, J. P.; Ruzsinszky, A.; Csonka, G. I.; Vydrov, O. A.; Scuseria, G. E.; Constantin, L. A.; Zhou, X.; Burke, K. *Phys. Rev. Lett.* **2008**, *100*, 136406. (d) Perdew, J. P.; Ruzsinszky, A.; Csonka, G. I.; Vydrov, O. A.; Scuseria, G. E.; Constantin, L. A.; Zhou, X.; Burke, K. *Phys. Rev. Lett.* **2009**, *102*, 039902. (e) van Lenthe, E.; Baerends, E. J.; Snijders, J. G. *J. Chem. Phys.* **1993**, *99*, 4597. (f) van Lenthe, E.; Baerends, E. J.; Snijders, J. G. *J. Chem. Phys.* **1994**, *101*, 9783. (g) van Lenthe, E.; Ehlers, A. E.; Baerends, E. J. *J. Chem. Phys.* **1999**, *110*, 8943. (h) Grimme, S.; Anthony, J.; Ehrlich, S.; Krieg, H. *J. Chem. Phys.* **2010**, *132*, 154104.

(18) Adams, R. D.; Kan, Y.; Rassolov, V.; Zhang, Q. *J. Organomet. Chem.* **2013**, *730*, 20–31.

(19) Csonka, G. I.; Ruzisinsky, A.; Perdew, J. P.; Grimme, S. *J. Chem. Theory Comput.* **2008**, *4*, 888–891.

(20) (a) Koitz, R.; Soini, T. M.; Genest, A.; Trickey, S. B.; Rosch, N. *J. Chem. Phys.* **2008**, *137*, 034102. (b) Johansson, M. P.; Lechtken, A.; Schooss, D.; Kappes, M. M.; Furche, F. *Phys. Rev. A: At., Mol., Opt. Phys.* **2008**, *77*, 053202.

DOI: 10.1021/acs.inorgchem.8b03201
Inorg. Chem. 2019, 58, 2109–2121